Oscar Salas; Herman Castañeda; Jesús De León-Morales
Attitude observer-based robust control for a twin rotor system

Kybernetika, Vol. 49 (2013), No. 5, 809--828

Persistent URL: `http://dml.cz/dmlcz/143527`

KYBERNETIKA — VOLUME 49 (2013), NUMBER 5, PAGES 809–828

ATTITUDE OBSERVER-BASED ROBUST CONTROL FOR A TWIN ROTOR SYSTEM

Oscar Salas, Herman Castañeda and Jesus De Leon-Morales

In this paper, an angular tracking control based on adaptive super twisting algorithm (ASTA) for a Twin Rotor System is presented. With the aim of implementing the ASTA control and taking into consideration the difficulties of measuring some of its states, a Nonlinear Extended State Observer (NESO) is employed to estimate the vector state and furthermore unmeasured dynamics. This scheme increases robustness against unmodeled dynamics and external disturbance, reducing modeling difficulties due to the fact that it is not necessary to know all the parameters of the system. Furthermore, an analysis of stability is provided, where sufficient conditions are given in order to guarantee the stability of the closed-loop system. Experimental results demonstrate the feasibility of the control scheme and illustrate its performance under external disturbance.

Keywords: robust adaptive control, extended state observer, flight control

Classification: 93E12, 62A10

1. INTRODUCTION

Helicopter control has been a major issue in nonlinear systems control theory owing to its high nonlinearity, noisy measurements and complicated dynamics including air flow, coupling and blade dynamics. Contrary to conventional real-size helicopters where the aerodynamic force is controlled using the propeller blade angle, in the twin rotor system setup (see Figure 1) the blades of the rotors have a fixed angle of attack. For this reason, the control is achieved by controlling the speeds of the rotors, therefore the voltages that regulates the speeds of the rotors are the only control inputs.

The control of 2-DOF helicopters has been investigated under algorithms ranging from linear robust control to nonlinear control domains [12, 16]. A nonlinear tracking control developed by [4] is based on state-space generalized predictive control, the control has a wide operating range, however there is no guarantee of stability. The main drawback of model-based control approaches resides in the helicopter dynamic model variations and uncertainties.

Traditional sliding modes control is used in many applications; in nonlinear plants it enables high gain accuracy tracking and insensitivity to disturbances and plant parameter variations. A controller based on sliding mode technique is the super-twisting control algorithm, which is designed to converge in a finite-time and ensures robustness under uncertainties. However, this controller needs to know the bounds of uncertainties and perturbations present on the system. In [2], 2-sliding mode techniques have been implemented in elevation and azimuth dynamics, however, tracking references were kept at constant values which reduces considerably cross-coupling dynamics effects. Adaptive Super Twisting Control represents an alternative to deal with uncertainties as it is not necessary to know their bounds. It has been successfully tested on a 3-DOF helicopter platform (see [17]). Nonetheless, the used experimental setup differs from the 2-DOF platform as the gyroscopic effects are canceled on tandem rotor configurations and furthermore is structurally constrained. The disturbance caused by gyroscopic effects is usually avoided as it leads to a dependence of the system on rotary frequency, for example quadrotor design intentionally circumvent its influence [24]. The fixed angle of attack of the rotor blades on the Twin Rotor platform adds an extra coupling caused by the reaction of the force necessary to change the propeller speed, instead of removing any of the essential couplings present on a conventional helicopter that need to be illustrated (see [15] for more details). Additionally, it tends to be a non minimum phase system exhibiting unstable zero dynamics [3].

On the other hand, with the aim of implementing a controller, information of the states of the system is necessary. However, it is not always possible to measure the states. This difficulty can be overcome by means of the use of observers, which estimates the states of the system from systems inputs and outputs. Before to design an observer, it is necessary to verify the observability of the system. Observability of nonlinear systems depends on the input. There exist inputs that render the system unobservable, which are called singular inputs. However, there exists a class of system which is observable for any input, this class of systems are called uniformly observable. Nonlinear systems which are uniformly observable can be transformed via a suitable change of coordinates into a canonical form with a triangular structure. There exist different kind of observers for uniformly observable systems, such as observers based on sliding modes techniques, which have a finite time convergence. Those based on high-gain with asymptotic convergence. A class of high-gain observer is the Extended State Observer, which have a remarkable performance to deal with dynamic uncertainties, disturbances, sensor noise and furthermore it is simple to tune [5, 20, 23]. In this case, parametric uncertainties and unmodeled dynamics of the system are considered as an additional state variable. Then, the perturbation can be compensated by canceling its estimate and thus each subsystem is controlled by a stand-alone controller.

This paper deals with the angular tracking of the twin rotor aerodynamic system. To solve the angular tracking control problem, an adaptive super twisting control algorithm is proposed. Moreover, in order to implement such controller, information about unmeasurable states is necessary. Then, a nonlinear extended state observer is proposed for estimating the required unmeasurable states, as well as parametric uncertainties and external disturbances. Furthermore, stability of the closed-loop system is demonstrated, where sufficient conditions are given. The performance of the proposed scheme is illustrated through experimental results.

The layout of this paper is as follows: In section 2, the problem statement and a system description containing a mathematical model of a Twin Rotor helicopter with 2-DOF are briefly introduced. In section 3 an Adaptive Super-Twisting Control is derived with the aim of providing robustness under parametric uncertainties and unmodeled dynamics. Moreover, in order to estimate the angular speed as well as external disturbances, a Nonlinear Extended State Observer is presented in section 4. In section 5 the stability in closed-loop of the proposed scheme is proven. Experimental results are given in section 6, to illustrate the effectiveness of the proposed scheme. Finally, conclusions of this work are drawn.

2. SYSTEM DESCRIPTION

The Twin Rotor platform consists of a beam pivoted on its base in such a way that it can rotate freely both in the horizontal and vertical planes (Figure 1). At both ends of the beam there are rotors (main and tail rotors) driven by DC motors. A counterbalance arm with a load at its end is fixed to the beam at the pivot. The state of the beam is described by four process variables: horizontal and vertical angles (ψ, θ) measured by position sensors fitted at the pivot, and two corresponding angular velocities ($\dot{\psi}$, $\dot{\theta}$). Two additional state variables are the angular velocities of the rotors (ω_h, ω_v, for tail and main rotor respectively), measured by tacho-generators coupled to the motors.

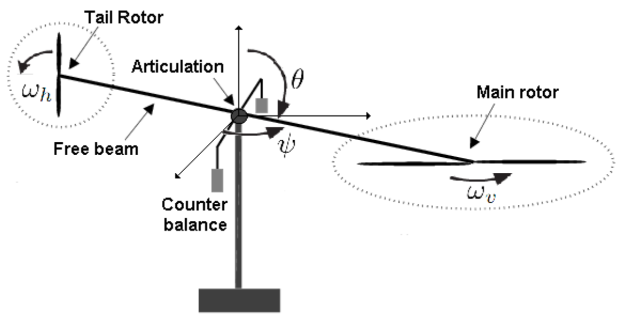

Fig. 1: The twin rotor system.

A dynamical model of a 2-DOF helicopter can be written as follows

$$
\begin{array}{l}
\Sigma_1 : \left\{ \begin{array}{lcl} \ddot{\theta} & = & \frac{1}{J_v}(l_m k_{Fv}\omega_v + k_{hv}u_2 - R_v\theta - k_{fv}\dot{\theta}), \\ \dot{\omega}_v & = & \frac{1}{\mu_1}(u_1 - \frac{\omega_v}{k_{Hv}}), \end{array} \right. \\
\Sigma_2 : \left\{ \begin{array}{lcl} \ddot{\psi} & = & \frac{1}{J_h}\{\mathsf{c}_\theta l_t\,[k_{Fh}\omega_h + k_{vh}u_1] - k_{fh}\dot{\psi} - \theta\mathsf{s}_\theta\,[k_{vh}u_1 + l_t k_{Fh}]\}, \\ \dot{\omega}_h & = & \frac{1}{\mu_2}(u_2 - \frac{\omega_h}{k_{Hh}}), \end{array} \right.
\end{array}
\tag{1}
$$

where k_{Hh}, k_{Hv}, k_{Fh}, k_{Fv} represent the velocity and thrust coefficients of the rotors, they are determined by linearization from the corresponding rotor static characteristics. k_{fh}, k_{fv} are the friction coefficients in the vertical and horizontal axes. k_{hv}, k_{vh} are the coefficients of the rotor cross moments. μ_1, μ_2 represent the moments of inertia of the set rotor-propeller. l_m, l_t correspond to the length from pivot to main and tail rotors, respectively. Furthermore, the system inputs are u_1 and u_2, corresponding to the voltage supplied to main and tail rotors respectively. $\mathtt{s}_{(\cdot)} = sin(\cdot)$, $\mathtt{c}_{(\cdot)} = cos(\cdot)$. The gain R_v, related to the coefficient of the returning torque corresponding to gravity forces, is described by the equation $R_v = k_1\mathtt{s}_\theta - k_2\mathtt{c}_\theta$, for constants k_1, k_2. J_v is the sum of moments of inertia with respect to the horizontal axis. The inertial moment around vertical axis, J_h, is denoted by the following equation $J_h = k_3\mathtt{c}_\theta^2 + k_4$, where the constants k_3, k_4 are determined by mass and geometric measures of the physical setup. More details about the parameters can be found in [1].

Taking the dynamics of the whole system (1) into account, it will be partitioned in two subsystems as follows: First subsystem, represented by $\Sigma_1(\theta, \dot{\theta}, \omega_v)$, consists of the big propeller which drives the rotation in vertical plane. Second subsystem, $\Sigma_2(\psi, \dot{\psi}, \omega_h)$, consists of the small propeller driving the angular rotation in horizontal plane.

Now, based on physical considerations, we introduce the following assumptions:

Assumption A1. The moments of inertia of the rotors (μ_1, μ_2), are negligible with respect to rigid body inertias (J_v, J_h) (see [13]). i. e.

$$(\mu_1, \mu_2) \ll (J_v, J_h).$$

According to **(A1)**, the dynamics of subsystems (Σ_1, Σ_2) can be represented in two time scales [9, 10], as follows.

- *Fast dynamic* represents the actuator dynamics, i. e. motor-propeller groups.
- *Slow dynamic* corresponds to the pitch and azimuth dynamics of the helicopter.

Then, a mathematical model of a Twin Rotor helicopter can be represented by the following MIMO singular perturbed form

$$\dot{\chi}_{i1} = \chi_{i2}, \tag{2a}$$
$$\dot{\chi}_{i2} = \mathtt{f}_i(\chi_1, \chi_2) + \mathtt{h}_i(\chi_1)\zeta_i + \mathtt{g}_i(\chi_1)u_i, \tag{2b}$$
$$\mu_i\dot{\zeta}_i = \bar{\mathtt{h}}_i\zeta_i + u_i, \qquad i = 1, 2, \tag{2c}$$

where $\chi_i = (\chi_{i1}, \chi_{i2})^T$, for $i = 1, 2$; represents the state vector of the slow subsystems (2a–2b) such as $\chi_1 = (\theta, \dot{\theta})^T$, $\chi_2 = (\psi, \dot{\psi})^T$, while rotor speeds dynamic $\zeta_1 = \omega_v$ and $\zeta_2 = \omega_h$ correspond to the fast subsystem (2c). $\mathtt{f}_1(\cdot) = -\frac{1}{J_v}[R_v\chi_{11} + k_{fv}\chi_{12}]$, $\mathtt{f}_2(\cdot) = -\frac{1}{J_h}[k_{fh}\chi_{22} + l_tk_{Fh}\mathtt{s}_{\chi_{11}}\chi_{11}]$, $\mathtt{h}_1(\cdot) = (l_mk_{Fv})/J_v$, $\mathtt{h}_2(\cdot) = \frac{1}{J_h}[l_tk_{Fh}\mathtt{c}_{\chi_{11}}]$, $\mathtt{g}_1(\cdot) = k_{hv}/J_v$, $\mathtt{g}_2(\cdot) = \frac{k_{vh}}{J_h}\left[\mathtt{c}_{\chi_{11}} - \mathtt{s}_{\chi_{11}}\chi_{11}\right]$, $\bar{\mathtt{h}}_1 = -1/k_{Hv}$, $\bar{\mathtt{h}}_2 = -1/k_{Hh}$.

Taking into account the magnitude of the moment of inertia of the rotors, whose experimental values satisfy

$$\mu_i \ll 1, \;\; i = 1, 2;$$

several methods can be applied to reduce the order of the model.

The classic quasy-steady-state represents a simple approach [21]. By applying this technique, the rotor speeds can be taken as approximately constant and as a result only the slow dynamics (θ, ψ) from (2a–2c) will be considered. Thus, setting $\mu_i = 0$, in the fast dynamic subsystem, it follows that $0 = \bar{\mathtt{h}}_i\zeta_i + u_i$, for $i = 1, 2$. Solving last equation for ζ_i and substituting in (2b), we obtain the *Slow System*

$$\left\{ \begin{array}{lcl} \dot{\chi}_{i1} & = & \chi_{i2}, \\ \dot{\chi}_{i2} & = & \mathtt{f}_i(\chi_1, \chi_2) + G_i(\chi_1)u_i + w_i(\chi_1, u_1, u_2), \quad i = 1, 2, \end{array} \right. \tag{3}$$

where $G_1(\chi_1) = \frac{l_m k_{Fv} k_{Hv}}{J_v}$, $G_2(\chi_1) = l_t k_{Fh} k_{Hh}$, $w_1(\chi_1, u_1, u_2) = \frac{k_{hv}}{J_v} u_2$, $w_2(\chi_1, u_1, u_2) = \frac{k_{vh}}{J_h} \{\mathtt{c}_{\chi_{i1}} - \mathtt{s}_{\chi_{i1}} \chi_{i1}\} u_1 + l_t k_{Fh} k_{Hh} (\mathtt{c}_{\chi_{i1}} / J_h) u_2$.

It is clear that, due to parameters variations and uncertainties, model (2a–2c) is an approximation of the behavior of the whole system. Accurate models can be found in literature, e. g. [19]. However, its derivation is not a trivial issue and requires a considerable effort.

From assumption **A1**, the subsystems (3), in the state space representation, can be written as

$$\Sigma_i : \left\{ \ \dot{\chi}_i = \mathcal{F}_i(\chi_i) + \mathcal{G}_i u_i, \qquad i = 1, 2, \right. \tag{4}$$

where $\mathcal{F}_i(\chi_i) = (\chi_{i2}, F_i(\chi_i))^T$ and $\mathcal{G}_i = (0, G_i)^T$, for $i = 1, 2$. Furthermore, u_i represents the motor voltage input, $F_i(\chi_i) = \mathtt{f}_i(\chi_i) + w_i(\chi_i)$, include dynamics, parametric uncertainties and external disturbances lumped together, for each subsystem, while G_i is a constant vector.

Assumption A2. The angles θ, ψ and rotor speeds ω_v, ω_h are the measurable outputs. Angular velocities $\dot{\theta}, \dot{\psi}$, are assumed to be unmeasurable, and terms F_i, for $i = 1, 2$; are unknown.

Then, in order to implement the proposed control laws, the terms $F_i, i = 1, 2$; will be estimated by means of extended state observers.

Now, we can establish the control and observation objectives.

Control objective. To design a controller able to track a desired angular reference (θ_d, ψ_d), regardless of uncertainties in modelling and crossed dynamics.

Observation objective. Considering that the only available measurements are the angular positions, the observation objective is to reconstruct the angular velocities and the uncertain terms of the system.

3. ADAPTIVE SUPER–TWISTING CONTROL ALGORITHM

In this section, the synthesis of control law based on a super-twisting adaptive control algorithm, which has been proposed in [22], is presented. Under this approach, the gains of the controller are adapted in order to attenuate the chattering. Furthermore, the bounds of uncertainties and perturbations present on the system are not required to be known. The main advantage of such algorithm is that it combines the advantage of the chattering reduction and the robustness of the high order sliding mode approach. The designed controller ensures its convergence in a finite-time and ensures the robustness of the system under uncertainties.

Now, consider the super-twisting control algorithm (see [11]), which is given by

$$\begin{aligned} u &= -K_1|s|^{1/2}\text{sign}(s) + v, \\ \dot{v} &= -K_2\text{sign}(s), \end{aligned} \tag{5}$$

where u represents the control signal, K_1, K_2 are the control gains and s is a sliding variable.

From the adaptive super-twisting control algorithm (ASTA) approach, the gains K_1 and K_2 are chosen such that they are functions of the sliding surface dynamics as follows

$$K_1 = K_1(t, s, \dot{s}) \quad \text{and} \quad K_2 = K_2(t, s, \dot{s}). \tag{6}$$

Now, in order to design an adaptive super-twisting control for the uncertain nonlinear system

$$\dot{x} = f(x, t) + g(x, t)u, \tag{7}$$

where $x \in \Re^n$ is the state, $u \in \Re$ the control input, $f(x, t) \in \Re^n$ is a continuous function.

We introduce the following assumptions.

Assumption B1. The sliding variable $s = s(x, t) \in \Re$ is designed so that the desired compensated dynamics of the system (7) are achieved in the sliding mode $s = s(x, t) = 0$.

Assumption B2. The relative degree of the system (7), with respect to control variable u, is equal to 1 and the internal dynamics are stable.

Then, the dynamics of the sliding variable s is given by

$$\dot{s} = a(x, t) + b(x, t)u, \tag{8}$$

where $a(x, t) = \frac{\partial s}{\partial t} + \frac{\partial s}{\partial x} f(x, t)$, $b(x, t) = \frac{\partial s}{\partial x} g(x)$.

Assumption B3. The function $b(x, t) \in \Re$ is unknown and different from zero $\forall x$ and $t \in [0, \infty)$. Furthermore, $b(x, t) = b_0(x, t) + \Delta b(x, t)$, where $b_0(x, t)$ is the nominal part of $b(x, t)$ which is known, and there exists γ_1 an unknown positive constant such that $\Delta b(x, t)$ satisfies

$$\left| \frac{\Delta b(x, t)}{b_0(x, t)} \right| \leq \gamma_1.$$

Assumption B4. There exist δ_1, δ_2 unknown positive constants such that the function $a(x, t)$ and its derivative are bounded

$$|a(x, t)| \leq \delta_1 |s|^{1/2}, \quad |\dot{a}(x, t)| \leq \delta_2. \tag{9}$$

The objective of ASTA approach is to design a continuous control without overestimating the gain, to drive the sliding variable s and its derivative $\dot{s}$ to zero in finite time, under bounded additive and multiplicative disturbances with unknown bounds γ_1, δ_1 and δ_2.

Then, the closed loop system (8) becomes

$$\begin{aligned} \dot{s} &= a(x,t) - K_1 b(x,t)|s|^{1/2}\mathrm{sign}(s) + b(x,t)\upsilon, \\ \dot{\upsilon} &= -K_2 \mathrm{sign}(s). \end{aligned} \tag{10}$$

Now, consider the following change of variable

$$\varsigma = (\varsigma_1, \varsigma_2)^T = (|s|^{1/2}\,\mathrm{sign}(s), b(x,t)\upsilon + a(x,t))^T. \tag{11}$$

Then, the system (10) can be written as

$$\dot{\varsigma} = \tilde{A}(\varsigma_1)\varsigma + \tilde{g}(\varsigma_1)\bar{\varrho}(x,t), \tag{12}$$

where

$$\tilde{A}(\varsigma_1) = \frac{1}{2\,|\varsigma_1|}\begin{pmatrix} -2b(x,t)K_1 & 1 \\ -2b(x,t)K_2 & 0 \end{pmatrix}, \qquad \tilde{g}(\varsigma_1) = \begin{pmatrix} 0 \\ 1 \end{pmatrix},$$

and $\bar{\varrho}(x,t) = \dot{b}(x,t)\upsilon + \dot{a}(x,t) = 2\varrho(x,t)\frac{\varsigma_1}{|\varsigma_1|}$. To prove the closed loop stability of the system,

Assumption B5. $\dot{b}(x,t)\upsilon$ is bounded with unknown boundary δ_3, i.e. $|\ \dot{b}(x,t)\upsilon\ | < \delta_3$.

Then, system (12) can be rewritten as follows

$$\dot{\varsigma} = \bar{A}(\varsigma_1)\varsigma \qquad \bar{A}(\varsigma_1) = \frac{1}{2\,|\varsigma_1|}\begin{pmatrix} -2b(x,t)K_1 & 1 \\ -2b(x,t)K_2 + 2\varrho(x,t) & 0 \end{pmatrix}, \tag{13}$$

where $|\varsigma_1| = |s|^{1/2}$, it is appealing to consider the quadratic function

$$V_0 = \varsigma^T \tilde{P}\varsigma, \tag{14}$$

where $\tilde{P}$ is a constant, symmetric and positive matrix, as a strict Lyapunov candidate function for (5). Taking its derivative along the trajectories of (13), we have

$$\dot{V}_0 = -\,|s|^{-1/2}\,\varsigma^T\tilde{Q}\varsigma, \tag{15}$$

almost everywhere, where $\tilde{P}$ and $\tilde{Q}$ are related by the Algebraic Lyapunov Equation

$$\bar{A}^T\tilde{P} + \tilde{P}\bar{A} = -\tilde{Q}. \tag{16}$$

Since $\bar{A}$ is Hurwitz if $b(x,t)K_1 > 0$, $2b(x,t)K_2 + 2\varrho(x,t) > 0$, for every $\tilde{Q} = \tilde{Q}^T > 0$, there exist a unique solution $\tilde{P} = \tilde{P}^T > 0$ for (16), so that V_0 is a strict Lyapunov function.

Remark 1. The stability of the equilibrium $\varsigma = 0$ of (13) is completely determined by the stability of the matrix $\bar{A}$. However, classical versions of Lyapunov's theorem [6] cannot be used since they require a continuously differentiable, or at least locally Lipschitz continuous Lyapunov function, though V_0 (19) is continuous but not locally Lipschitz. Nonetheless, as it is explained in Theorem 1 in [14], it is possible to show the convergence properties by means of Zubov's theorem [18], that requires only continuous Lyapunov functions. This argument is valid in all the proofs of the present paper, so that no further discussion of these issues will be required.

From Assumption B4 and B5, it follows that

$$0 < \varrho(x,t) < \delta_2 + \delta_3 = \delta_4.$$

Notice that, while ς_1 and ς_2 converge to 0 in finite time, it follows that s and $\dot{s}$ converge to 0 in finite time, too.

The control design based on ASTA approach is formulated in the following theorem.

Theorem 3.1. (Shtessel et al. [22]) Consider the system (7) in closed-loop with the control (5), expressed in terms of the sliding variable dynamics (8). Furthermore, the assumptions $B1 - B5$ for unknown gains $\gamma_1, \delta_1, \delta_2 > 0$ are satisfied. Then, for given initial conditions $x(0)$ and $s(0)$, there exists a finite time $t_F > 0$ and a parameter ι, as soon as the condition

$$K_1 > \frac{(\lambda + 4\epsilon_*)^2 + 4\delta_4^2 + 4\delta_4(\lambda - 4\epsilon_*^2)}{16\epsilon_*\lambda},$$

holds, if $|s(0)| > \iota$, so that a real 2-sliding mode, i. e. $|s| \leq \eta_1$ and $|\dot{s}| \leq \eta_2$, is established $\forall t \geq t_F$, under the action of Adaptive Super-Twisting Control Algorithm (5) with the adaptive gains

$$\begin{aligned} \dot{K}_1 &= \begin{cases} \omega_1\sqrt{\dfrac{\gamma_1}{2}}\operatorname{sign}(|s| - \iota), & \text{if } K_1 > K_*, \\ K_*, & \text{if } K_1 \leq K_*, \end{cases} \\ K_2 &= 2\epsilon_* K_1, \end{aligned} \tag{17}$$

where $\epsilon_*, \lambda, \gamma_1, \omega_1, \iota$ are arbitrary positive constants, and $\eta_1 \geq \iota$, $\eta_2 > 0$.

Proof. For analyzing the stability analysis of the closed loop system (13), consider the following Lyapunov function candidate

$$V(\varsigma, K_1, K_2) = V_0 + \sum_{i=1}^{2}\{\frac{1}{2\gamma_i}(K_i - K_i^*)^2\}, \tag{18}$$

where

$$V_0 = \varsigma^T \tilde{P} \varsigma, \quad \text{with} \quad \tilde{P} = \begin{pmatrix} \lambda + 4\epsilon_*^2 & -2\epsilon_* \\ -2\epsilon_* & 1 \end{pmatrix}, \tag{19}$$

and $\lambda, \epsilon_*, \gamma_2, K_1^*$ and $K_2^* > 0$. Notice that the matrix $\tilde{P}$ is positive definite if $\lambda > 0$ and $\epsilon_* \in \Re$.

Then, the symmetric matrix $\tilde{Q}$ is given by

$$\tilde{Q} = \frac{1}{2\,|s|^{\frac{1}{2}}} \begin{pmatrix} 4b(x,t)\left[K_1(\lambda + 4\epsilon_*^2) - 2K_2\epsilon_*\right] + 8\rho\epsilon_* & * \\ -\lambda - 4\epsilon_*^2 - 2b(x,t)\left[2K_1\epsilon_* - K_2\right] - 2\rho & 4\epsilon_* \end{pmatrix}. \tag{20}$$

By selecting

$$K_2 = 2\epsilon_* K_1, \tag{21}$$

then, from assumptions $B3 - B5$, it is easy to see that the matrix $\tilde{Q}$ will be positive definite with a minimal eigenvalue $\lambda_{\min}(\tilde{Q}) \geq 2\epsilon_*$ if

$$K_1 > \frac{(\lambda + 4\epsilon_*)^2 + 4\delta_4^2 + 4\delta_4(\lambda - 4\epsilon_*^2)}{16\epsilon_*\lambda\gamma_1}. \tag{22}$$

Now, taking the time derivative of the Lyapunov function candidate (18) along the trajectories of (13), it follows that

$$\dot{V}(\varsigma, K_1, K_2) = \dot{V}_0 + \sum_{i=1}^{2} \frac{1}{\gamma_i}(K_i - K_i^*)\dot{K}_i, \tag{23}$$

where

$$\dot{V}_0 = \varsigma^T\{\tilde{A}(\varsigma_1)^T\tilde{P} + \tilde{P}\tilde{A}(\varsigma_1)\}\varsigma \leq -\frac{1}{|\varsigma_1|}\varsigma^T\tilde{Q}\varsigma. \tag{24}$$

Since $\tilde{Q}$ is positive definite with a minimal eigenvalue $\lambda_{\min}(\tilde{Q}) \geq 2\epsilon_*$, the following inequality is satisfied

$$\dot{V}_0 \leq -\frac{1}{|\varsigma_1|}\varsigma^T\tilde{Q}\varsigma \leq -\frac{2\epsilon_*}{|\varsigma_1|}\|\varsigma\|^2, \tag{25}$$

and, from the norm equivalence, we have

$$\lambda_{\min}(\tilde{P})\|\varsigma\|^2 \leq \varsigma^T\tilde{P}\varsigma \leq \lambda_{\max}(\tilde{P})\|\varsigma\|^2, \tag{26}$$

where $\|\varsigma\|^2 = |s| + \varsigma_2^2$, and

$$|\varsigma_1| = |s|^{1/2} \leq \|\varsigma\| \leq \sqrt{\frac{V_0(\varsigma)}{\lambda_{\min}(\tilde{P})}}.$$

Then, choosing a suitable selection of the gains according to (21),(22), it follows that

$$\dot{V}_0 \leq -rV_0^{1/2}, \quad r = 2\epsilon_*\frac{\sqrt{\lambda_{\min}(\tilde{P})}}{\lambda_{\max}(\tilde{P})}. \tag{27}$$

From equations (23) and (27), we have

$$\dot{V}(\varsigma, K_1, K_2) \quad \leq \quad -rV_0^{1/2} + \textstyle\sum_{i=1}^{2} \frac{1}{\gamma_i}\epsilon_{Ki}\dot{K}_i^*, \tag{28}$$

where $\epsilon_{Ki} = (K_i - K_i^*)$ for i=1,2. By adding $\pm\sum_{i=1}^{2}\{\frac{\omega_i}{\sqrt{2\gamma_i}}\,|\epsilon_{Ki}|\}$ to (28), it follows that

$$\dot{V}(\varsigma, K_1, K_2) \;\leq\; -rV_0^{1/2} - \textstyle\sum_{i=1}^{2} \frac{\omega_i}{\sqrt{2\gamma_i}}\,|\epsilon_{Ki}| + \sum_{i=1}^{2}\left\{\frac{1}{\gamma_i}\epsilon_{Ki}\dot{K}_i^* + \frac{\omega_i}{\sqrt{2\gamma_i}}\,|\epsilon_{Ki}|\right\}. \tag{29}$$

Since $(x^2+y^2+z^2)^{\frac{1}{2}} \leq |x|+|y|+|z|$, the following inequality holds

$$-rV_0^{1/2} - \sum_{i=1}^{2} \frac{\omega_i}{\sqrt{2\gamma_i}} |\epsilon_{Ki}| \leq -\eta_0 \sqrt{V(\varsigma, K_1, K_2)}, \tag{30}$$

with $\omega_2 > 0$, $\eta_0 = \min(r, \frac{\omega_1}{\sqrt{2\gamma_1}}, \frac{\omega_2}{\sqrt{2\gamma_2}})$. According to the inequality (30), the equation (28) can be rewritten as

$$\dot{V}(\varsigma, K_1, K_2) \leq -\eta_0 \sqrt{V(\varsigma, K_1, K_2)} + \sum_{i=1}^{2} \left\{ \frac{1}{\gamma_i} \epsilon_{Ki} \dot{K}_i^* + \frac{\omega_i}{\sqrt{2\gamma_i}} |\epsilon_{Ki}| \right\}. \tag{31}$$

Now, recalling on the definition of the adaptive gains (17), a solution in the domain $\iota < |s| \leq \eta_1$ can be constructed as

$$K_1 = K_1(0) + \omega_1 \sqrt{\frac{\gamma_1}{2}} t, \quad 0 \leq t \leq t_F. \tag{32}$$

K_1 is thus bounded. As $K_2 = 2\epsilon_* K_1$, the adaptive gain K_2 is also bounded.

Inside the domain $|s| \leq \iota$, the control gains K_1 and K_2 are decreasing. Therefore, the gains K_1 and K_2 are bounded in the real 2-sliding mode.

Then, there exist positive constants K_1^*, K_2^* such that $K_i - K_i^* < 0$, $\forall \geq 0$, $i = 1, 2$. Therefore, the equation (31) can be reduced to

$$\dot{V}(\varsigma, K_1, K_2) \leq -\eta_0 \sqrt{V(\varsigma, K_1, K_2)} + \widehat{\epsilon}, \tag{33}$$

where

$$\widehat{\epsilon} = -\sum_{i=1}^{2} |\epsilon_{Ki}| \left(\frac{1}{\gamma_i} \dot{K}_i - \frac{\omega_i}{\sqrt{2\gamma_i}} \right).$$

Then, if $|s| > \iota$ and $K_1 > K_1^*, \forall t \geq 0$, it follows that

$$\dot{K}_1 = \omega_1 \sqrt{\tfrac{\gamma_1}{2}} \quad \text{and} \quad \widehat{\epsilon} = -|\epsilon_{K2}| \left(\tfrac{1}{\gamma_2} \dot{K}_2 - \tfrac{\omega_2}{\sqrt{2\gamma_2}} \right). \tag{34}$$

Thus, by selecting $\epsilon_* = \frac{\omega_2}{2\omega_1} \sqrt{\frac{\gamma_2}{\gamma_1}}$, we have

$$\dot{K}_2 = \omega_2 \sqrt{\frac{\gamma_2}{2}}. \tag{35}$$

From (35), the term $\widehat{\epsilon}$ in (33) becomes $\widehat{\epsilon} = 0$, it follows that

$$\dot{V}(\varsigma, K_1, K_2) \leq -\eta_0 \sqrt{V(\varsigma, K_1, K_2)}. \tag{36}$$

Integrating (36), we have

$$\sqrt{V(t, \varsigma, K_1, K_2)} \leq \sqrt{V(t_0, \varsigma, K_1, K_2)} - \frac{\eta_0}{2} t. \tag{37}$$

Let $\sqrt{V(t_0, \varsigma, K_1, K_2)} - \frac{\eta_0}{2} t_F = 0$, then the convergence time t_F is given by

$$t_F = \frac{2\sqrt{V(t_0, \varsigma, K_1, K_2)}}{\eta_0}. \tag{38}$$

Therefore, for $t > t_F$ we have $V(t) = 0$.

On the other hand, when $|s| < \iota$, K_1 is given by (17), and the term $\widehat{\epsilon}$ becomes

$$\widehat{\epsilon} \;=\; \begin{cases} 2\left|K_1 - K_1^*\right| \frac{\omega_1}{\sqrt{2\gamma_1}}, & \text{for } K_1 > K_*, \\ -\left|K_* - K_1^* + \eta t\right| \left(\frac{\eta}{\gamma_1} - \frac{\omega_1}{\sqrt{2\gamma_1}}\right), & \text{for } K_1 \le K_*. \end{cases} \tag{39}$$

Therefore, during the adaptation process the sliding variable s reaches the domain $|s| \le \iota$ in finite time. If s leaves the domain for a finite time, it is guaranteed that it will holds in a larger domain $|s| \le \eta_1, \eta_1 > \iota$ in a real sliding mode.

Within the domain $|s| \le \iota$, the value $|\dot{s}|$ can be estimated according to system (10) and from gain equations (17) – (21) as

$$|\dot{s}| \le \left\{(1-\gamma_1)K_1 + \delta_1\right\} \iota^{\frac{1}{2}} + 2\epsilon_* K_1 (1-\gamma_1)(t_2 - t_1) = \bar{\eta}_1, \tag{40}$$

where t_1, t_2 are the time when s enters and leaves the domain $|s| \le \iota$, respectively.

If $\iota < |s| \le \eta_1$, similarly we have

$$|\dot{s}| \le (1+\gamma_1)(\sqrt{\eta_1} + \epsilon_*)(K_1(t_2) + \omega_1 \sqrt{\frac{\eta_1\gamma_1}{2}})(t_3 - t_2) + \delta_1 \sqrt{\eta_1} = \bar{\eta}_2, \tag{41}$$

where $t_2, t_3, t_3 > t_2$, are the time instants when s leaves and enters the domain $|s| \le \iota$ respectively.

From these conditions (40) – (41), we obtain

$$|\dot{s}| \le \max(\bar{\eta}_1, \bar{\eta}_2) = \eta_2, \tag{42}$$

and thus is proved the existence of the real sliding mode domain

$$W = \left\{s, \dot{s} : |s| \le \eta_1, |\dot{s}| \le \eta_2, \eta_1 > \iota\right\}. \tag{43}$$

This ends the proof. □

Notice that, according to subsystems (4), the sliding surface for the control (5) – (6) is defined as

$$s = \begin{bmatrix} s_1 \\ s_2 \end{bmatrix} = \begin{bmatrix} \left(\chi_{12} - \dot{\theta}_d(t)\right) + \lambda_1 \left(\chi_{11} - \theta_d(t)\right) \\ \left(\chi_{22} - \dot{\psi}_d(t)\right) + \lambda_2 \left(\chi_{21} - \psi_d(t)\right) \end{bmatrix}, \tag{44}$$

whose time derivatives are given by

$$\dot{s} = \begin{pmatrix} \left\{F_1 - \ddot{\theta}_d(t) + \lambda_1\left(\chi_{12} - \dot{\theta}_d(t)\right)\right\} + b_1 v_1 \\ \left\{F_2 - \ddot{\psi}_d(t) + \lambda_2\left(\chi_{22} - \dot{\psi}_d(t)\right)\right\} + b_2 v_2 \end{pmatrix} = \begin{pmatrix} a_1 + b_1 v_1 \\ a_2 + b_2 v_2 \end{pmatrix} \tag{45}$$

where $(\theta_d(t), \psi_d(t))$ are the desired angular trajectories and (v_1, v_2) the control inputs defined according to (5) – (17).

However, to implement the proposed controller, it is necessary to know the values from (χ_{12}, χ_{12}), as well as the unknown dynamics of F_i, for i=1,2. Then, to overcome this difficulty, the estimation of unmeasurable terms will be addressed in next section.

4. NONLINEAR EXTENDED STATE OBSERVER DESIGN

In this section, a Nonlinear Extended State Observer (NESO) is designed for estimating angular velocities $\dot{\theta}, \dot{\psi}$ and unknown terms F_i in subsystems (Σ_1, Σ_2). In order to design such observer, subsystems (4) are first extended into the following form

$$\widetilde{\Sigma}_i : \begin{cases} \dot{\chi}_{i1} &= \chi_{i2} \\ \dot{\chi}_{i2} &= \chi_{i3} + b_{i0} u_i \\ \dot{\chi}_{i3} &= \eta_i(\chi) \\ y &= \chi_{i1}, \qquad i = 1, 2, \end{cases} \tag{46}$$

where b_{i0} represents nominal value of b_i, with $b_i = b_{i0} + \Delta b_i$ and the additional states $\chi_{i3} = F_i(\chi_i) + \frac{\Delta b_i}{b_{i0}} u_i$ are the augmented states, estimating the total disturbance for every subsystem.

Assumption C1. $F_i(\cdot)$, u_i and theirs derivative $\eta_i(\cdot) = \dot{F}_i(\chi_i) + \frac{\Delta b_i}{b_{i0}} \dot{u}_i$, $i = 1, 2$; are locally Lipschitz in their arguments and bounded within the domain of interest. Besides, the initial conditions are assumed as $F(\cdot)|_{t=0} = 0$, and $\dot{F}_i(\cdot)|_{t=0} = 0$.

Assumption C2. The output $y_i = \chi_{i1}$, for $i = 1, 2$; and its derivatives up to 4th order are bounded.

Then, the following system

$$O_i : \begin{cases} \dot{z}_{i1} &= z_{i2} - \beta_{i1} fal(\hat{e}_{i1}(t), \hat{\gamma}_{i1}, \hat{\delta}_i), \\ \dot{z}_{i2} &= z_{i3} - \beta_{i2} fal(\hat{e}_{i1}(t), \hat{\gamma}_{i2}, \hat{\delta}_i) + b_{i0} u_i, \\ \dot{z}_{i3} &= -\beta_{i3} fal(\hat{e}_{i1}(t), \hat{\gamma}_{i3}, \hat{\delta}_i), \qquad i = 1, 2, \end{cases} \tag{47}$$

is an observer estimating the unmeasurable states of (46), where $\hat{e}_{ij}(t) = \chi_{ij} - z_{ij}$ for $j = 1, 2, 3$; is the estimation error, $\beta_i = (\beta_{i1}, \beta_{i2}, \beta_{i3})^T$ are the observer gains and $Z_i = (z_{i1}, z_{i2}, z_{i3})^T$, for $i = 1, 2$; is estimation state vector for each subsystem (46).

The function $fal(\cdot)$ is defined as follows

$$fal(e, \hat{\gamma}, \hat{\delta}) = \begin{cases} |e|^{\hat{\gamma}} \operatorname{sign}(e), & |e| > \hat{\delta}, \\ \frac{e}{\hat{\delta}^{1-\hat{\gamma}}}, & |e| \leq \hat{\delta}, \end{cases} \tag{48}$$

where $\hat{\gamma}$ and $\hat{\delta}$ are design parameters.

The nonlinear function (48) is used to increase the rate of convergence of the signals. As $\hat{\gamma}$ is chosen between 0 and 1, $fal(\cdot)$ yields high gain when error is small, while large errors correspond to smaller gains. If $\hat{\gamma}$ is chosen as unity, then the observer is equal to the well-know Luenberger observer. $\hat{\delta}$ is a small number used to limit the gain in the neighborhood of origin (see Figure 2). Starting with linear gain $fal(\cdot) = e$, the pole placement method can be used for the initial design of this observer (see [7]), before the nonlinearities are added to enhance the performance.

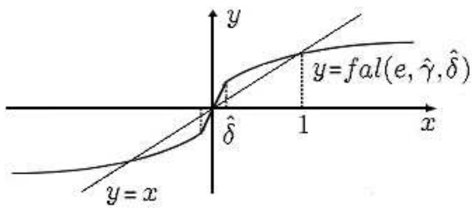

Fig. 2: Linear and nonlinear gains comparison.

Several analytical techniques can be used to find the parameters $\beta_{i1}, \beta_{i2}, \beta_{i3}$, of the observer. To simplify, the poles of characteristic equation are placed in one location ($\widehat{\omega}_i$) and the observer gains can be expressed as

$$\beta_{ij} = l_{ij}\widehat{\omega}_i^j, \; i = 1, 2; \; j = 1, 2, 3; \tag{49}$$

where the parameters $l_{ij}, \; i = 1, 2; \; j = 1, 2, 3;$ are selected such that the characteristic polynomial $s^3 + l_{i1}s^2 + l_{i2}s + l_{i3}$ is Hurwitz. $\widehat{\omega}_i > 0$ is a design parameter, the bandwidth of the output signal of the observer. It is common to choose the parameter $\widehat{\omega}_i$ as a trade-off between convergence speed of states estimation and the influence of noise and sampling time. A study of the convergence of this observer is given in [8].

5. STABILITY OF THE CONTROLLER-OBSERVER SCHEME

In section 3, the controller has been designed considering that the states are available for measurement. However, in practice it is not possible to measure all components of the state of the system, then the observer provided the estimates which converge near of the actual state. In order to guarantee the correct performance of the proposed observer-controller scheme a stability analysis of the system in closed-loop is necessary.

Consider the case for subsystems (4) where the control depends on the estimated state

$$\dot{\chi}_i \quad = \quad \mathcal{F}_i(\chi_i) + \mathcal{G}_i u_i(Z_i),$$

where $\mathcal{F}_i(\chi_i) = (\chi_{i2}, F_i(\chi_i))^T$ and $\mathcal{G}_i = (0, b_i)^T$, for $i = 1, 2$. Adding the term $\pm\mathcal{G}_i u_i(\chi_i)$, the system can be represented as follows

$$\dot{\chi}_i \quad = \quad \mathcal{F}_i(\chi_i) + \mathcal{G}_i u_i(\chi_i) + \mathcal{G}_i \left[u_i(Z_i) - u_i(\chi_i)\right], \quad i = 1, 2. \tag{50}$$

Using the sliding mode surface (44), then the derivatives of the sliding variables $s = (s_1, s_2)^T$ can be written as

$$\dot{s} = \mathcal{A}(\chi) + \mathcal{B}(\chi)u(\chi) + \Gamma(\epsilon), \tag{51}$$

where $\mathcal{A}(\chi) = [a_1(\chi_1, t), a_2(\chi_2, t)]^T$, $\mathcal{B}(\chi) = diag\,[b_1(\chi_1), b_2(\chi_2)]$, $\Gamma(\epsilon) = [\Gamma_1(\epsilon_1), \Gamma_2(\epsilon_2)]^T$, $a_i(\chi_i, t) = \frac{\partial s_i}{\partial t} + \frac{\partial s_i}{\partial \chi_i}\mathcal{F}_i(\chi_i)$, $b_i(\chi_i, t) = \frac{\partial s_i}{\partial \chi_i}\mathcal{G}_i$, $u(\chi) = (u_1(\chi_1), u_2(\chi_2))^T$, $\Gamma_i(\epsilon) = b_i(\chi_i)\,[u_i(Z_i) - u_i(\chi_i)]$. Furthermore, $\Gamma_i(\epsilon)$ for $i = 1, 2$; depend on the estimation errors $\epsilon_i = Z_i - \chi_i$, for $i = 1, 2$;, and from theorem 2, they are bounded.

On the other hand, the terms $a_i(\chi_i, t)$ and $b_i(\chi_i, t)$, $i = 1, 2$ satisfy Assumptions B3 and B4. Then, under these assumptions, system (51) in closed-loop with the control (5) − (6) is given by

$$\begin{array}{rcll} \dot{s}_i & = & -\kappa_{1i}|s_i|^{1/2}\mathrm{sign}(s_i) + v_i + \Gamma_i(\epsilon_i), & \\ \dot{v}_i & = & -\kappa_{2i}\mathrm{sign}(s_i), & i = 1, 2, \end{array} \tag{52}$$

where $\kappa_{1i} = K_{1i}b_i$, $\kappa_{2i} = \frac{K_{2i}}{2}b_i$.

Using the following change of variable $\xi_i = (\mid s_i \mid^{1/2} \mathrm{sign}(s_i), \quad v_i + a_i(\chi_i, t))^T$, the system (50) is given by

$$\begin{array}{rcll} \dot{\xi}_{i1} & = & -\frac{1}{2|s_i|^{1/2}}\{\kappa_{1i}b_i(\chi_i, t)\xi_{i1} + \xi_{i2} + \Gamma_i(\epsilon_i)\}, & \\ \dot{\xi}_{i2} & = & -\frac{1}{2|s_i|^{1/2}}\{\kappa_{2i}\xi_{i1} + \dot{a}_i(\chi_i, t)\}, & i = 1, 2. \end{array} \tag{53}$$

Consider the following Lyapunov function

$$V_i = \xi_i^T \bar{P}_i \xi_i, \quad \text{where} \quad \bar{P}_i = \frac{1}{2}\begin{pmatrix} 4\kappa_{2i} + \kappa_{1i}^2 & -\kappa_{1i} \\ -\kappa_{1i} & 2 \end{pmatrix}, \qquad i = 1, 2. \tag{54}$$

Now, the time derivative of the Lyapunov function (54) is given by

$$\dot{V}_i = -\frac{1}{|s_i|^{1/2}}\xi_i^T Q_i \xi_i + \frac{\Gamma_i(\epsilon_i)}{|s_i|^{1/2}} q_{1i}^T \xi_i, \tag{55}$$

where

$$Q_i = \frac{\kappa_{1i}}{2}\begin{pmatrix} 2\kappa_{2i} + \kappa_{1i}^2 & -\kappa_{1i} \\ -\kappa_{1i} & 1 \end{pmatrix}, \qquad q_{1i} = \begin{pmatrix} 2\kappa_{2i} + \frac{1}{2}\kappa_{1i}^2 \\ -\frac{1}{2}\kappa_{1i} \end{pmatrix}.$$

Following the same procedure as defined in [14], the term $\Gamma_i(s_i, \epsilon_i)$ is assumed to be globally bounded, i. e.

$$\mid \Gamma_i \mid \leq \rho_i \mid s_i \mid^{1/2}, \qquad \rho_i > 0.$$

Then, it follows that

$$\dot{V}_i \leq -\frac{\kappa_{1i}}{2|s_i^{1/2}|}\xi_i^T \tilde{Q}_i \xi_i, \quad \tilde{Q}_i = \begin{pmatrix} 2\kappa_{2i} + \kappa_{1i}^2 - \left(\frac{4\kappa_{2i}}{\kappa_{1i}}\right)\rho_i & -\kappa_{1i} + 2\rho_i \\ -\kappa_{1i} + 2\rho_i & 1 \end{pmatrix}. \tag{56}$$

Thus, if the controller gains satisfy the next relations

$$\kappa_{1i} > 2\rho_i, \qquad \kappa_{2i} > \kappa_{1i}\frac{5\rho_i\kappa_{1i} + 4\rho_i^2}{2(\kappa_{1i} - 2\rho_i)}. \tag{57}$$

According to Theorem 3.1 and taking into account the asymptotically convergence from the term Γ_i, a K_{1i} can be designed such that the following condition holds

$$K_{1i} > 2b_i\rho_i, \qquad \frac{K_{2i}}{2} > K_{1i}\frac{5\rho_i\kappa_{1i} + 4\rho_i^2}{2(\kappa_{1i} - 2\rho_i)}. \tag{58}$$

Since $\tilde{Q}_i > 0$, implies the derivative of the Lyapunov function is negative definite.

6. EXPERIMENTAL RESULTS

In this section, we provide experimental results carried out on the *Two Rotor Aerodynamical System (TRAS)* platform (Figure 3) to illustrate the effectiveness of the proposed methodology. The TRAS system is interfaced through an external PC-based data

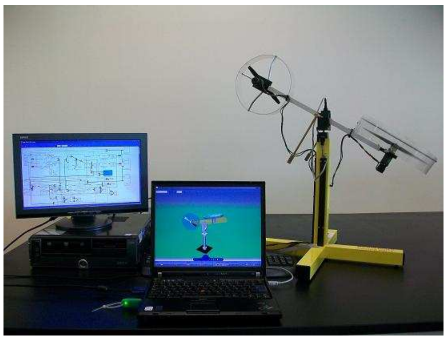

Fig. 3: Experimental platform.

acquisition and control system (RT-DAC4/USB). Controller and observer algorithms were developed in the MATLAB/Simulink environment, while the associated executable code was automatically generated by the RTW/RTWI rapid prototyping environment (see [1] for detailed information). The sampling time was set to $0.01s$.

Controller and observer parameters are displayed in the Tables $1-2$. Regarding the *Control parameters:* $\omega_i, \iota_i, \epsilon_{*I}$ and γ_i are positive values arbitrary chosen between 0 and 1. λ_i, is a positive value related to the sliding surface derivative action. With respect to *Observer parameters:* $\hat{\delta}_i$ and $\hat{\gamma}_{ij}, i = 1,2; j = 1,2,3$; are arbitrary chosen between 0 and 1. b_{0i} is related to motor-propeller time constant. $\beta_{ij}, i = 1,2; j = 1,2,3$; are selected according to (49), where $\hat{\omega_i}, i = 1,2$; were selected as a trade-off between convergence speed and noise sensibility. Finally, parameters $l_{ij}, i = 1,2; j = 1,2,3$; were selected as $l_{i1} = 3$, $l_{i2} = 3$ and $l_{i3} = 1, i = 1,2$. In the first test, a sinusoidal reference of amplitude 0.2 rad with a frequency of 1/60Hz was given for pitch angle, while for azimuth angle a square reference of amplitude 0.4 rad with a frequency of 1/50Hz was chosen. In the second test, an extra weight of 25% has been attached to the main rotor 20 seconds after the beginning of the experiments, i. e. 15 grams have been added to observe the response under the perturbation aforementioned. In order to compare the performance of the NESO based ASTA scheme, a Cross-coupled PID and the fixed gain Super Twisting Algorithm (STA) using the estimates states from NESO were also tested.

Subsystem	ω_i	λ_i	ι_i	γ_i	ϵ_{*i}
Pitch (i=1)	0.1	1	0.1	0.1	0.1
Azimuth (i=2)	0.1	3	0.1	0.1	0.1

Tab. 1: ASTA Control parameters.

Subsystem	$\hat{\gamma}_{i1}$	$\hat{\gamma}_{i2}$	$\hat{\gamma}_{i3}$	$\hat{\delta}_i$	b_{0i}	β_{i1}	β_{i2}	β_{i3}
Pitch (i=1)	0.5	0.35	0.25	0.15	0.001	67.5	1518.8	11391
Azimuth (i=2)	0.5	0.35	0.25	0.1	0.005	30	300	1000

Tab. 2: Extended Observer parameters.

Figure 4 shows profiles of angular responses. From the graphics it is possible to see that the strong coupling in the dynamics has been rejected by the proposed controllers. In Figure 6 can be seen the resulting speed on azimuth rotor, Figure 5 shows the corresponding main rotor speed, the profiles show a bigger demand by the proposed controller. However, tracking is preserved despite coupled dynamics. An error comparison is shown in Figure 7. Additionally, in Figure 8 adaptation of ASTA gain is presented, where gains for azimuth and pitch were initialized with different values. While for the rest of the graphics the time scale remains fixed to 90 seconds to make easier to observe the details of responses, for gain graphics the time scale has been extended in order to show the convergence. In the above graphics it is possible to see that, the controller ASTA in combination with NESO can reject the strong coupled dynamics of the platform TRAS. Several indexes of performance in the Table 3 illustrate the advantage of NESO based ASTA scheme.

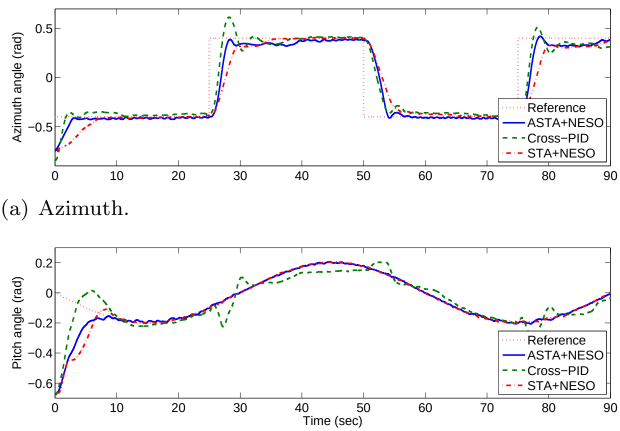

(a) Azimuth.

(b) Pitch.

Fig. 4: State responses for first test.

Angular profiles under an increment of rotor mass are showed in Figure 9, it can be observed that for pitch tracking, Cross-PID control totally lost the reference, while az-

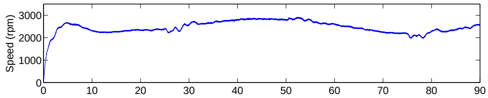

(a) Cross-PID.

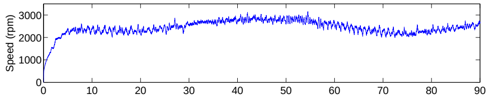

(b) NESO based ASTA.

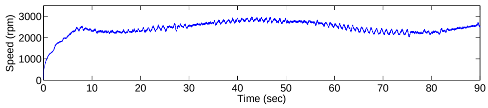

(c) NESO based STA.

Fig. 5: Main rotor speed for first test.

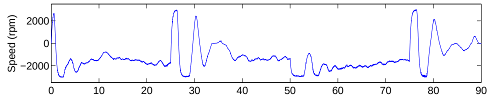

(a) Cross-PID.

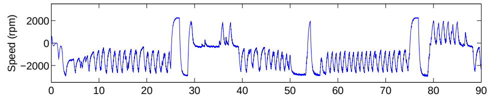

(b) NESO based ASTA.

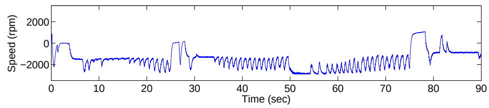

(c) NESO based STA.

Fig. 6: Tail rotor speed for first test.

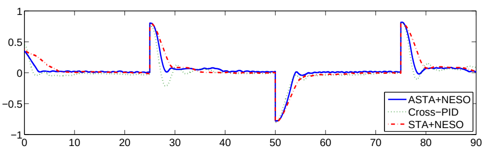

(a) Azimuth error.

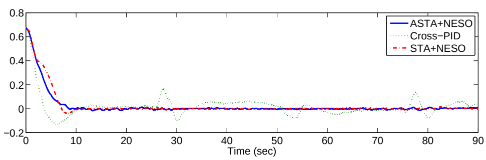

(b) Pitch error.

Fig. 7: First test errors.

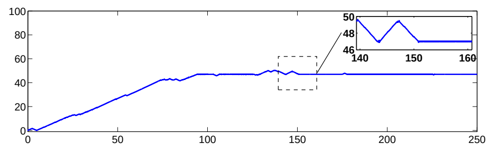

(a) Azimuth gain.

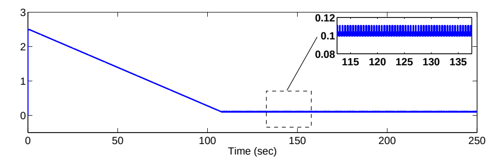

(b) Pitch gain.

Fig. 8: First test adaptive gains.

imuth tracking is reached by all the controllers. To prevent any damage to the platform, the control outputs are saturated, this can be observed as azimuth angle can not reject faster the perturbation as it has reached its saturation value. By increasing the mass of pitch rotor, controllers demand more performance, as can be seen in Figures 10 − 11. In the Figure 12 an error comparison for second test is presented. As Cross-PID control is unable to handle the increment of mass, it has a huge tracking error. Adaptive gains of the ASTA controller help to reject the perturbation applied to the 2-DOF helicopter. Figure 13 shows the behavior of the ASTA gains, from the extended time scale it is possible to see their convergence. According to performance indexes displayed in the Table 4, the proposed scheme present the best performance among the tested controllers.

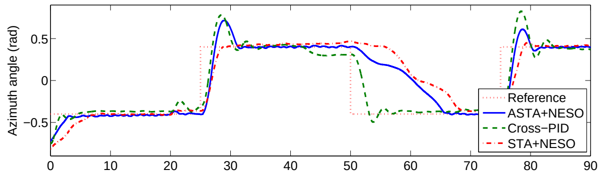

(a) Azimuth.

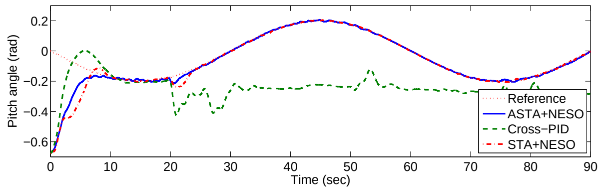

(b) Pitch.

Fig. 9: State responses for second test.

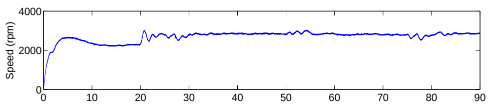

(a) Cross-PID.

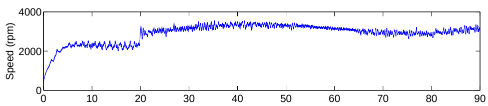

(b) NESO based ASTA.

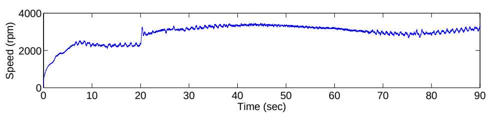

(c) NESO based STA.

Fig. 10: Main rotor speed for second test.

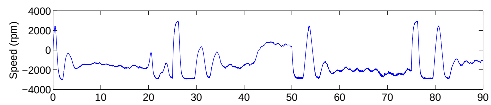

(a) Cross-PID.

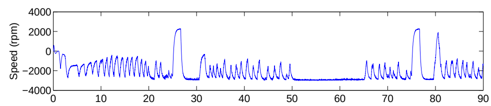

(b) NESO based ASTA.

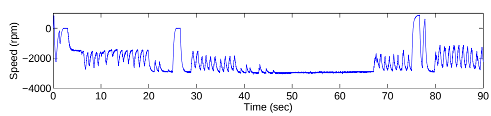

(c) NESO based STA.

Fig. 11: Tail rotor speed for second test.

7. CONCLUSIONS

An adaptive super-twisting control algorithm for a two degrees of freedom laboratory helicopter platform has been designed. With the aim of implementing the proposed controller, a nonlinear extended state observer was designed for estimating the unmeasurable states as well as external disturbances. An analysis of the stability of the system has been given, where sufficient conditions have been defined in order to guarantee the stability of the closed loop. Besides, a comparison among a Cross-PID and the Super Twisting Algorithm illustrate the advantages of the presented scheme. Experimental results demonstrate the robustness and the efficiency of the proposed methodology.

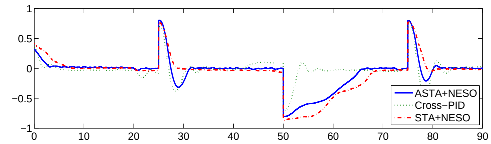

(a) Azimuth error.

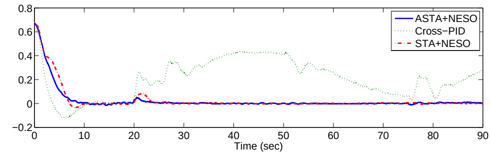

(b) Pitch error.

Fig. 12: Second test errors.

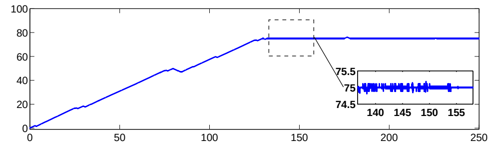

(a) Azimuth gain.

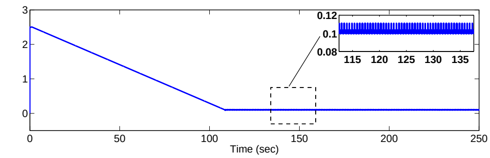

(b) Pitch gain.

Fig. 13: Second test adaptive gains.

	MSE[a]	ITAE[b]	$\|u\|_2$
Pitch control			
NESO based ASTA	0.009	1916.645	47.284
Cross-PID	0.009	14126.229	43.566
NESO based STA	0.011	1947.061	44.712
Azimuth control			
NESO based ASTA	0.038	37010.961	26.288
Cross-PID	0.032	36919.345	17.175
NESO based STA	0.051	47395.427	24.971

Tab. 3: First test performance.

	MSE	ITAE	$\|u\|_2$
Pitch control			
NESO based ASTA	0.009	1963.227	64.207
Cross-PID	0.067	89474.449	50.119
NESO based STA	0.012	1971.801	59.954
Azimuth control			
NESO based ASTA	0.070	62079.431	27.598
Cross-PID	0.031	40080.065	18.817
NESO based STA	0.100	81159.385	27.152

Tab. 4: Second test performance.

[a]Mean Square Error.
[b]Integral Time Absolute Error.

(Received February 27, 2013)

REFERENCES

[1] Anon1: Two Rotor Aero-dynamical System. User's manual. Inteco Ltd., 2006.

[2] Q. Ahmed, A. Bhatti, S. Iqbal, and I. Kazmi: 2-sliding mode based robust control for 2-dof helicopter. In: 11th Internat. Workshop on Variable Structure Systems 2010, pp. 481–486.

[3] M. Azam and S. N. Singh: Invertibility and trajectory control for nonlinear maneuvers of aircraft. J. Guidance, Control and Dynamics *17* (1998), 1, 192–200.

[4] A. Dutka, A. Ordys and M. Grimble: Non-linear predictive control of 2 dof helicopter model. In: Proc. 42nd IEEE Conference on Decision and Control 2003.

[5] L. B. Freidovich and H. K. Khalil: Performance recovery of feedback-linearization-based designs. IEEE Trans. Automat. Control *53* (2008), 10, 2324–2334.

[6] A. Filippov: Differential Equation with Discontinuos Right-Hand Side. Kluwer 1988.

[7] Z. Gao: Scaling and bandwidth – parametrization based controller tuning. In: IEEE Proc. American Control Conference, Denver 2003, pp. 4989–4996.

[8] B. Z. Guo and Z. L. Zhao: On convergence of non-linear extended state observer for multi-input multi-output systems with uncertainty. IET Control Theory Appl. *6* (2012), 15, 2375–2386.

[9] H. K. Khalil: Nonlinear Systems. Prentice Hall, Englewood Cliffs, NJ 2002.

[10] P. V. Kokotovic and H. K. Khalil: Singular Perturbation Methods in Control: Analysis and Design. Academic Press, London 1986.

[11] A. Levant: High-order sliding modes, differentiation and output-feedback control. Internat. J. Control *76* (2003), 9–10, 924–941.

[12] M. Lopez-Martinez and F. Rubio: Approximate feedback linearization of a laboratory helicopter. In: Proc. 6th Portuguese Conference on Automatic Control 2004, pp. 43–48.

[13] M. Lopez-Martinez, M. Ortega, C. Vivas, and F. Rubio: Nonlinear L_2 control of a laboratory helicopter with variable speed rotors. Automatica *43* (2007), 4, 655–661.

[14] J. Moreno and M. Osorio: Strict Lyapunov functions for the super-twisting algorithm. IEEE Trans. Automat. Control *57* (2012), 4, 1035–1040.

[15] Ph. Mullhaupt, B. Srinivasan, J. Levine, and D. Bonvin: A Toy more difficult to control than the real thing. In: Proc. European Control Conference 1999, pp. 253–258.

[16] P. Petkov, N. Christov, and M. Konstatinov: Robust real-time control of a two-rotor aerodynamic system. In: Proc. 17th IFAC World Congress 2008, pp. 6422–6427.

[17] F. Plestan and A. Chriette: A robust controller based on adaptive super-twisting algorithm for a 3DOF helicopter. In: Decision and Control Conference 2012, pp. 7095–7100.

[18] A. S. Poznyak: Advanced Mathematical Tools for Automatic Control Engineers. Elsevier, Deterministic Techniques *1*, Amsterdam 2008, p. 774.

[19] A. Rahideh, M. Shaheed, and H. Huijberts: Dynamic modelling of a TRMS using analytical and empirical approaches. Control Engrg. Practice *16* (2008), 241–259.

[20] G. Reale, P. Ortner, and L. Del Re: Nonlinear observers for closed-loop control of a combustion engine test bench. In: Proc. 2009 American Control Conference *6*, Missouri 2009, pp. 4648–4653.

[21] V. Saksena, J. O'Reily, and P. Kokotovic: Singular perturbations and time-scale methods in control theory: Survey 1976 – 1983. Automatica *20* (1984), 273–293.

[22] Y. Shtessel, M. Taleb, and F. Plestan: A novel adaptive-gain supertwisting sliding mode controller: methodology and application. Automatica *48* (2012), 5, 759–769.

[23] X. Yang and Y. Huang: Capabilities of extended state observer for estimating uncertainties. In: Proc. American Control Conference *1*, Missouri 2009, pp. 3700–3705.

[24] B. Zhu and W. Huo: Trajectory linearization control for a quadrotor helicopter. In: 8th International Conference on Control and Automation 2010, pp. 34–39.

Oscar Salas, Department of Electrical Engineering, University of Nuevo Leon. México.
e-mail: salvador.sp@gmail.com

Herman Castañeda, Department of Electrical Engineering, University of Nuevo Leon. México.
e-mail: hermancc08@gmail.com

Jesús DeLeón-Morales, Department of Electrical Engineering, University of Nuevo Leon. México.
e-mail: drjleon@gmail.com